

# OPTICAL BEAM QUALITY ANALYSIS OF THE CLARA TEST FACILITY USING SECOND MOMENT ANALYSIS

H. M. Castañeda Cortés\*, D. J. Dunning, M. D. Roper and N. L. Thompson  
 ASTeC, Cockcroft Institute, STFC, Daresbury Laboratory, Warrington, United Kingdom

## Abstract

We studied and characterised the FEL optical radiation in simulations of the CLARA FEL test facility under development at Daresbury Laboratory in the UK. In particular, we determined the optical beam quality coefficient, waist position and other source properties corresponding to different potential FEL operating modes via wavefront propagation in free space using OPC (Optical Propagation Code) and second moment analysis. We were able to find the operation mode and undulator design for which the optical beam has the optimum quality at highest brightness. Furthermore, we studied the way that different properties of the electron bunches (emittance, peak current, bunch length) affect the optical beam. We are now able to understand how the optical beam will propagate from the end of the undulator and through the photon transport system to the experimental stations. This knowledge is necessary for the correct design of the photon transport and diagnostic systems.

## INTRODUCTION

The CLARA FEL test facility, currently under construction at Daresbury Laboratory [1], will have different operation modes in order to probe and test several advanced FEL concepts, such as high brightness SASE, mode-locking and afterburner schemes [2]. An aspect of fundamental interest in the design of CLARA is the assessment of the radiation properties obtained at the end of the FEL process. It is extremely important to optimise the design of the facility so that the optical beam quality does not degrade as the beam is transported through the optical beamline. This paper summarises the studies of optical beam quality carried out for the long bunch operation mode, assessing the different design parameters which could degrade or enhance it. The spatial source properties are calculated by using second moment analysis.

## SECOND MOMENT ANALYSIS

The  $M^2$  analysis states that the second moment of the optical beam profile follows a quadratic free-space propagation rule in terms of the propagating distance  $z$  as [3]

$$\sigma_i^2 = \sigma_{i0}^2 + \left( \frac{M_i^2 \lambda}{4\pi \sigma_{i0}} \right)^2 (z - z_0)^2, \quad \text{where } i = x, y. \quad (1)$$

The  $M^2$  parameter compares the beam quality of the propagated beam to the free-space propagation of a TEM<sub>00</sub> Gaussian beam ( $M_i^2 = 1$ ). The rms size at the beam waist is  $\sigma_{i0}$  and  $z_0$  the waist position.  $M_i^2$ ,  $\sigma_{i0}$  and  $z_0$  can be calculated

from fitting the evolution of the optical beam profile (defined as  $\sigma_i^2(z) = C_2 z^2 + C_1 z + C_0$ ) to the measured values of second moments, [4],

$$M_i^2 = \frac{2\pi}{\lambda} \sqrt{4C_0 C_2 - C_1^2}, \quad (2)$$

$$z_0 = -\frac{C_1}{2C_2}, \quad \text{and} \quad (3)$$

$$\sigma_{i0} = \sqrt{C_0 - \frac{C_1^2}{4C_2}}. \quad (4)$$

The optical code OPC [5, 6] was used to perform the free-space propagation of the calculated radiation at the end of the undulator. Time-dependent FEL simulations were carried out in GENESIS 1.3 [7] to obtain the radiation field.

## PRELIMINARY STUDY

The long bunch operation mode in CLARA is designed to demonstrate FEL schemes generating radiation pulses significantly shorter than the electron bunch length. It will have between 150 and 250 MeV beam energy, 250 pC bunch charge,  $\sigma_t = 800$  fs, peak current of 125 A, 0.5 mm-mrad normalised emittance and 25 keV energy spread. Planar variable gap undulators will have a 2.5 cm period and maximum rms of the undulator parameter of 1.4, allowing resonant wavelengths between 100 and 400 nm. A comparison of steady state and time-dependent simulations in GENESIS 1.3 was done to have a rough estimate of the source properties and demonstrate the validity of time-dependent approach for beam quality calculations. Previous CLARA undulator values were used, as given in Table 2. The radiation wavelength defined for the simulations is set to be 266 nm (the shortest wavelength for single-shot temporal diagnostics).

Table 1: Comparison Between Optical Beam Parameters Obtained from Steady State and Time-Dependent Simulations.

Parameter	Steady State		Time-Dependent	
	x	y	x	y
$M^2$	3.8	3.6	3.6	3.5
$z_0$ (m)	-1.85	-1.93	-1.27	-1.27
$\sigma_{z_0}$ (μm)	283	273	274	278

Second moment analysis was performed via the wavefront propagation code FOCUS (for steady state simulations) [8] and OPC (for time-dependent simulations). The obtained source properties for both scenarios (following Eqs. (2), (3), and (4)) are shown in Table 1. The  $M^2$  parameters obtained

\* hector.castaneda@stfc.ac.uk

Table 2: Undulator parameters chosen for the preliminary study in last section and each undulator module length case. There are 1.5 undulator periods end pieces for all cases, per end.

Parameter	Previous Study	Undulator module length		
		0.5 m	0.75 m	1 m
Und. period [m]	0.0275	0.025	0.025	0.025
Active periods	28	17	27	37
Number of periods drift	18	23	23	23
Break sections [m]	0.4125	0.5	0.5	0.5
Quad length [m]	0.055	0.05	0.05	0.05
x/y quad. gradient [T/m]	8/10	13/13	10/10	9/9

for the steady state and time-dependent simulations are quite close to each other with a relative difference of 5.2% and 2.8% in x and y, respectively. Therefore, the time-dependent simulations are suitable in order to find the radiation source properties. However, the  $M^2$  obtained for both steady state and time-dependent simulations deviates from  $M^2 = 1$ , corresponding to a TEM<sub>00</sub> Gaussian beam.

## IMPACT OF UNDULATOR MODULE LENGTH

As a follow-up to the previous study, three different undulator module lengths (0.5, 0.75 and 1 m) were chosen in order to find the radiation source properties for each undulator length (characterised by the number of undulator segments ( $n_{sec}$ ) in GENESIS 1.3). Table 2 shows the undulator parameters chosen for each simulated undulator module length (compared to the ones used in the previous section).

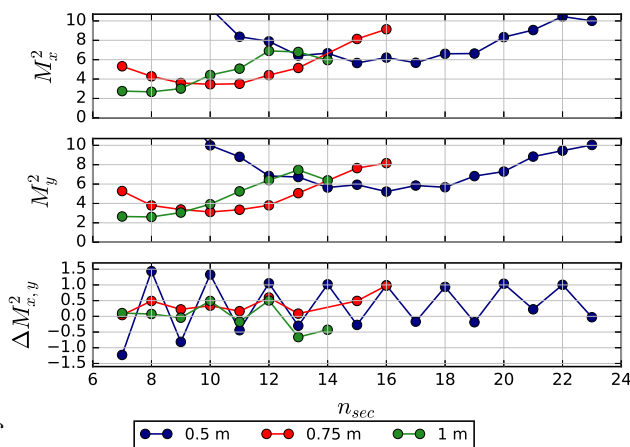


Figure 1:  $M^2$  in x (top) and y (middle) and their difference  $\Delta M_{x,y}^2 = M_x^2 - M_y^2$  (bottom) in terms of the number of undulator segments (for 0.5, 0.75 and 1 m modules).

Fig. 1 shows that a parabolic function can be fitted around the minimum value of  $M^2$  as a function of  $n_{sec}$  for the three

chosen modules. The minimum  $M^2$  coefficient for the 0.5 m module length (in Table 3) has the largest  $M^2$  of all modules (2.1 and 2.3 times larger than the smallest value obtained for the 1 m module in x and y, respectively). As it is desired to have a  $M^2$  as close to the TEM<sub>00</sub> Gaussian mode as possible for higher beam quality, this module can be discarded as a possibility.

The difference between  $M^2$  in x and y,  $\Delta M_{x,y}^2$ , (in Fig. 1) in terms of  $n_{sec}$  fluctuates around a non-zero value due to the focusing and defocusing of the electron beam while traversing the FODO cell. It shows an asymmetry in beam quality due to the difference in focusing for both transversal directions. For larger undulator lengths, the difference in focusing and defocusing is more significant (especially deep into saturation) and the difference in beam quality between x and y increases.

Table 3: Comparison Between Source Parameters at  $n_{sec}$  Corresponding to the Minimum of  $M^2$  for the Three Proposed Undulator Module Lengths

L (m)	$M_x^2$	$M_y^2$	$z_{0x}$ [m]	$z_{0y}$ [m]	$\sigma_{z_{0x}}$ [ $\mu$ m]	$\sigma_{z_{0y}}$ [ $\mu$ m]
0.5	5.65	5.93	-1.3	-1.19	350	351
0.75	3.46	3.12	-1.1	-1.11	229	229
1	2.68	2.6	-1.21	-1.1	202	211

To get a complete picture of how impactful the change in the undulator design is, we consider the beam brightness, defined in terms of the  $M^2$  coefficient as [9]

$$B_{x,y} = 16P_{n_{sec}} / (\lambda^2 (M_{x,y}^2)^2). \quad (5)$$

Here  $\lambda$  is the radiation wavelength and  $P_{n_{sec}}$  is the peak power at the end of the  $n_{sec}$  undulator segment.

It can be seen in Fig. 2 that the brightness has its maximum value at a number of undulator segments larger than the one that corresponds to the minimum  $M^2$ . We, therefore, choose the undulator length associated with the highest brightness as the most feasible comparison scenario for the three undulator modules. This case approximately corresponds to the onset of saturation of the FEL.

The results in Table 4 show the source properties calculated at the number of the undulator segments where the brightness is maximum. The 0.75 and 1 m modules have the best results at maximum brightness. When compared, the relative difference between the beam quality coefficients shows that the beam quality for those undulator modules is similar (relative difference less than 1% in x and 3.1% in y). The 0.75 m module is chosen for compatibility with the novel schemes to be tested in the facility, such as mode locking and HB-SASE.

## IMPACT OF BEAM PARAMETERS

Different electron beam scenarios were proposed to study the impact of electron beam properties on the beam quality: (A) Increased emittance bunch (from 0.5 to 0.8 mm-mrad),

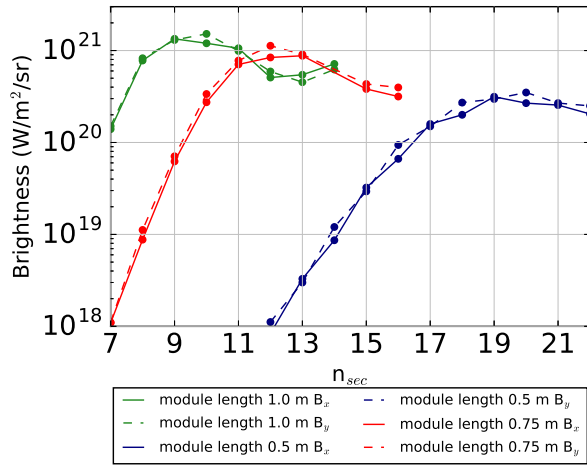


Figure 2: Brightness for the three undulator module lengths as a function of  $n_{sec}$ .

Table 4: Comparison Between Optical Beam Parameters at  $n_{sec}$  Corresponding to Maximum Brightness for the Three Proposed Modules

L (m)	$M_x^2$	$M_y^2$	$z_{0x}$ [m]	$z_{0y}$ [m]	$\sigma_{z_{0x}}$ [ $\mu$ m]	$\sigma_{z_{0y}}$ [ $\mu$ m]
0.5	8.32	7.29	-1.99	-2.1	509	471
0.75	4.40	3.80	-1.41	-1.50	300	287
1	4.41	3.92	-1.86	-1.97	348	329

(B) reduced quad strength (from 10 to 2 T/m, so that the electron beam is much bigger in one plane), (C) symmetric undulator focusing (by artificially setting the undulator to be helical in GENESIS 1.3, it can be guaranteed that the focusing in both planes will be the same) and (D) electron beam with double peak current and half the bunch length.

A summary of the calculated source properties for the  $n_{sec}$  at which  $M^2$  to be minimum and at which the brightness is maximum can be found in Table 5. The brightness as a function of number of undulator segments for each scenario is shown in Fig. 3.

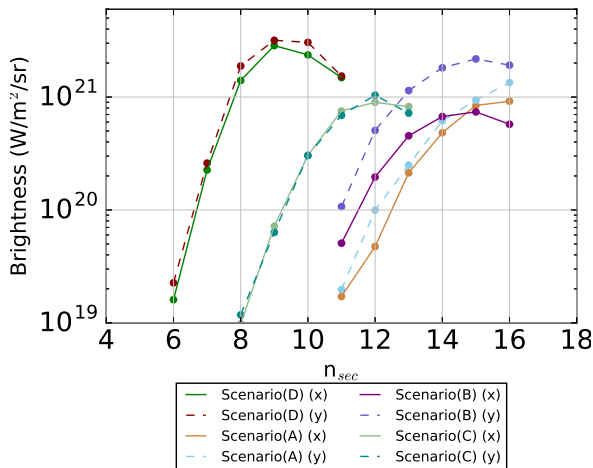


Figure 3: Brightness as a function of the undulator length (for the electron beam case studies).

Table 5: Optical Beam Parameters at  $n_{sec}$  Corresponding to the Minimum  $M^2$  and Maximum Brightness for the Electron Beam Scenario

Scenario	Minimum $M^2$		Maximum Brightness	
	$M_x^2$	$M_y^2$	$M_x^2$	$M_y^2$
Scenario (A)	3.61	3.34	4.65	3.86
Scenario (B)	3.67	2.31	4.76	2.77
Scenario (C)	3.54	3.57	4.41	4.11
Scenario (D)	3.04	2.69	3.38	3.21

Considering only the calculated values at maximum brightness, the comparison of  $M^2$  for the larger emittance scenario parameters shows degradation in the beam quality with respect to the nominal 0.75 m module (relative difference of  $M^2$  in x around 5.7% and 1.5% in y). The  $M^2$  parameter in y for the reduced quad strength scenario is the smallest of all considered proposals (2.77 for the y direction in Table 5), making the beam less divergent in that direction. The relative difference of  $M^2$  with respect to the nominal 0.75 m module case in x shows degradation in beam quality (around 8.2%) but an important improvement of beam quality in y (27%). The symmetric focusing scenario does not show any improvement of beam quality in either of the planes. The  $M^2$  is indeed more symmetric between the two planes. Finally, the electron beam with twice the peak current and half the bunch length has the minimum  $M^2$  of all proposed cases. When comparing the obtained parameters to the results in Table 4, an improvement in the beam quality is achieved, with a  $M^2$  reduced to 0.77 and 0.84 of the nominal case in x and y, respectively. Thus, the beam quality is improved for both planes. A large difference of the  $M^2$  in x and y shows an asymmetry in the beam profile. In particular, the reduced quad strength scenario favours the beam quality on one coordinate of the transversal plane (stronger focusing in one plane).

Similarly to that studied previously, the beam quality was assessed for undulator designs which produces coherent radiation with wavelength of 100 and 400 nm. The  $M^2$  at maximum brightness were calculated for the 100 nm and 400 nm. A slight improvement of beam quality in x and y can be observed for the 400 nm with respect to the nominal 0.75 m module length ( $M_x^2 = 4.28$  and  $M_y^2 = 3.38$  with relative difference of 2.7% and 11% in x and y, respectively). The 100 nm scenario shows improvement in beam quality for both transversal planes with respect to the 0.75 m module length, providing the best optical beam quality of the studied cases (2.87 and 2.77 in x and y respectively).

## SUMMARY

Following the second moment analysis, the beam quality coefficient  $M^2$  and main source properties were calculated for the long bunch mode at the CLARA test facility. Three different module lengths (0.5, 0.75 and 1 m) were assessed to determine the impact of the undulator design on the beam

quality. The source properties were determined per module as a function of the undulator length. The  $M^2$  parameter used for comparison was chosen to be the one corresponding to the undulator length at the largest brightness. It was shown that choosing an undulator module length of 0.75 m, optimum for the different R&D topics proposed, does not degrade the beam quality compared to longer modules.

## REFERENCES

- [1] J. A. Clarke *et al.*, “CLARA conceptual design report”, *JINST*, Vol. 9, pp. T05001, 2014.
- [2] D.J. Dunning, “CLARA Facility Layout and FEL Schemes”, presented at FEL2017, Santa Fe, USA, Aug. 2017, paper MOP054, this conference.
- [3] A. E. Siegman, “How to (Maybe) Measure Laser Beam Quality”, in DPSS (Diode Pumped Solid State) Lasers: Applications and Issues, M. Dowley, ed., Vol. 17 of OSA Trends in Optics and Photonics (Optical Society of America), paper MQ1, 1998.
- [4] M. D. Roper, “Matching a variable-included-angle grating monochromator to the properties of a soft X-ray FEL source to achieve a controlled temporal stretch”, *Nucl. Instrum. Methods A*, Vol. 635, pp. S80–S87, 2011.
- [5] J. Karssenberg *et al.*, “Modelling paraxial wave propagation in free-electron laser oscillators”, *J. App. Phys.*, Vol. 100, 093106, 2006.
- [6] P.J.M. van der Slot, “Recent Updates to the Optical Propagation code OPC”, in *Proceedings of the Int. FEL Conference Conf. (FEL'14)*, Basel, Switzerland, Aug. 2014, paper TUP021, pp. 412-415.
- [7] S. Reiche, “Genesis 1.3: a fully 3D time-dependent FEL simulation code”, *Nucl.Instrum.Methods A*, Vol. 429, pp. 243–248, 1999.
- [8] M.A. Bowler and S. P. Higgins, “FOCUS – A new Wavefront Propagation Code”, presented at the SMEXOS Conference, Grenoble, France, Feb. 2009, <http://www.esrf.eu/files/live/sites/www/files/events/conferences/2009/SMEXOS/talkBowler.pdf>.
- [9] G. Machavariani, N. Davidson, Y. Lumer, I. Moshe, A. Meir, and S. Jackel, “New methods of mode conversion and beam brightness enhancement in a high-power laser”, *Opt. Mater.*, Vol. 30, pp. 1723–1730, 2008.

Content from this work may be used under the terms of the CC BY 3.0 licence (© 2018). Any distribution of this work must maintain attribution to the author(s), title of the work, publisher, and DOI.